World Academy of Science, Engineering and Technology
International Journal of Structural and Construction Engineering
Vol:11, No:9, 2017

Effect of Scarp Topography on Seismic Ground Motion

Haiping Ding, Rongchu Zhu, Zhenxia Song

***Abstract*—**Local irregular topography has a great impact on earthquake ground motion. For scarp topography, using numerical simulation method, the influence extent and scope of the scarp terrain on scarp's upside and downside ground motion are discussed in case of different vertical incident SV waves. The results show that: (1) The amplification factor of scarp's upside region is greater than that of the free surface, while the amplification factor of scarp's downside part is less than that of the free surface; (2) When the slope angle increases, for x component, amplification factors of the scarp upside also increase, while the downside part decrease with it. For z component, both of the upside and downside amplification factors will increase; (3) When the slope angle changes, the influence scope of scarp's downside part is almost unchanged, but for the upside part, it slightly becomes greater with the increase of slope angle; (4) Due to the existence of the scarp, the z component ground motion appears at the surface. Its amplification factor increases for larger slope angle, and the peaks of the surface responses are related with incident waves. However, the input wave has little effects on the x component amplification factors.

***Keywords*—**Scarp topography, ground motion, amplification factor, vertical incident wave.

I. Introduction

TOPOGRAPHY has important influence on seismic ground motion. It is often found that earthquake damage at the mountain ridges, the escarpments, the high isolated hills, and the edge of scarp or slope is obviously severe. For instance, in 1966 Dongchuan, Yunnan earthquake, damage of a convalescent hospital, which was located at the upper edge of a hill, was more severe than that of the base. Besides, in 1970 Tonghai, Yunnan earthquake, villages located at the regional raised hills or ridges suffer more intensive destructions than the surrounding area. And in 1988 Lancang- Gengma, Yunnan earthquake, some multi-storey buildings at the top of isolated hills were destroyed, whereas the one storey houses almost had no damages [1]-[3]. The seismic records also show these characteristics. Using the aftershock records of the San Fernando earthquake, Davis and West [4] found that accelerations at the mountaintop were several times larger compared with that at the mountain base. The observed velocity records at the crest and base of Kagel Mountain showed that the duration time of seismic motion at the crest increased obviously, accompanying with significant amplification effects [5]. In 2008 Wenchuan earthquake, the records of the strong motion observatory array deployed at Zigong Xi-Shan Park showed that the PGA values of 7 bedrock stations generally increase from mountain base to top [6].

Besides field experiments, the analytical and numerical methods are another two main means to study the effect of topography on seismic ground motion. The analytical methods are mainly used in response studying of regular topographies, such as the semi-cylindrical and semi-elliptical canyons [7], [8], the semi-cylindrical and semi-elliptical alluvial valleys [9], [10], shallow circular cylindrical canyons [11], circular-arc shaped cylindrical hills [12], and shallow circular alluvial valleys [13] under incident plane SH waves; the semi-circular canyons under incident plane P waves [14]; the circular-arc alluvial valleys under incident plane P and SV waves [15], [16], etc. However, for irregular topography such as scarps, the analytical methods are not suitable, and the numerical methods are often used [17]-[19]. Ashford and Sitar [20], [21] investigated three parameters to quantify the topographic effects of steep slopes, i.e., the topographic amplification, the site amplification, and the apparent amplification.

In this study, numerical simulation method combining the finite element method and the multi-transmitting boundary condition is applied to investigate the effects of scarp topography on the seismic wave propagation and amplification behavior under vertical incident SV waves, and the influence range and degree of scarps with varying slope angle are discussed.

II. Calculation Model

Considering a homogeneous, isotropic, and elastic half-space with a scarp topography (Fig. 1). The elastic parameters are taken as: the shear wave velocity $v_s = 1000 m/s$, the mass density $\rho = 2700 kg/m^3$, and the Poisson ratio $\mu = 0.25$. The calculation model and the observation points are shown in Fig. 1, where point 1 are located at a distance of 100 m from the left boundary, and the intervals from point 1 to point 17 are 40 m. Smaller intervals of 20 m are used from points 17-25. Along the slope, points 25-29 are equally spaced. The intervals of points 29-37 and points 37-53 are 20 m and 40 m, respectively. The distance from points 53 to the right boundary is 100 m. The slope angle is chosen as 0°, 10°, 20°, 30°, 40°, 50°, separately.

The wave is vertically incident from the bottom of the model in a SV type, and the input waves are chosen as pulse wave, El-Centro wave and Ninghe wave, with the time histories shown in Figs. 2-4.

Haiping Ding, Rongchu Zhu and Zhenxia Song are with the Key Laboratory of Structure Engineering of Jiangsu Province, Suzhou University of Science and Technology, Suzhou 215011, China (e-mail: haiping_ding@sina.com).

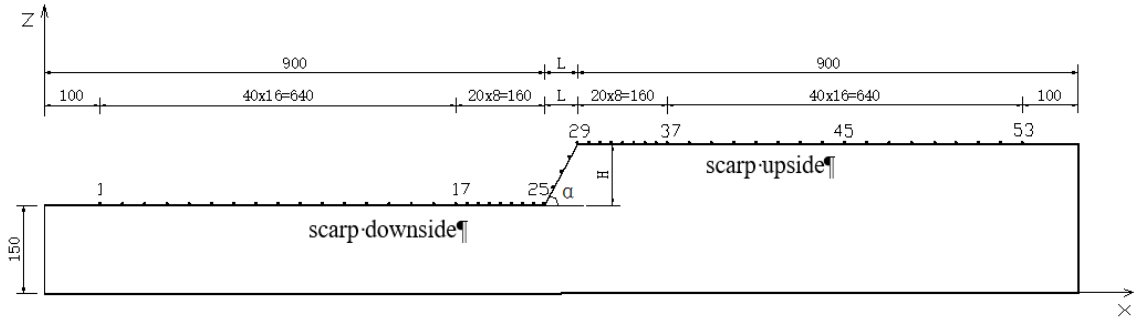

Fig. 1 Scarp model and the observers' position (units: m)

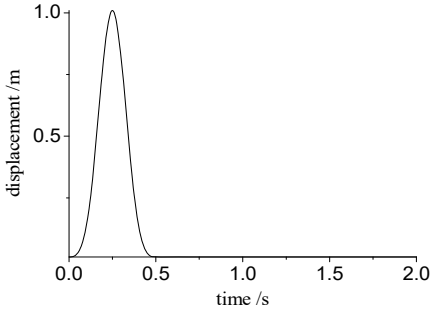

Fig. 2 Incident pulse waveform

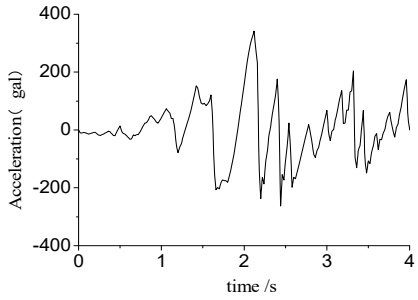

Fig. 3 Acceleration time history of incident EI-Centro wave (truncated from 0-4 s)

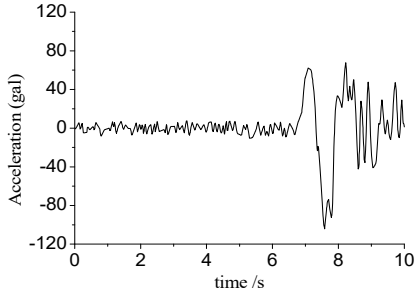

Fig. 4 Acceleration time history of incident Ninghe wave (truncated from 0-10 s)

III. Seismic Response of Free Surface of Scarp Model

Besides the slope angle, the slope width L and slope height H are also considered in the seismic motion simulation of scarp topography. And the seismic motion amplification factor (hereinafter referred to as amplification factor) β is defined as the ratio of the amplitude of free surface points to that of the input waves.

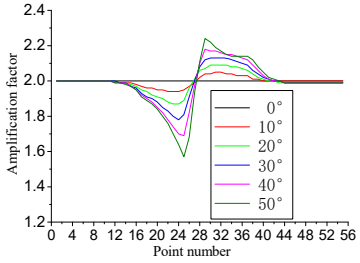

(a) Pulse wave

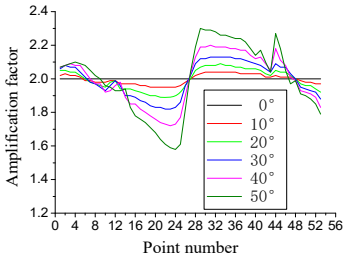

(b) El-Centro wave

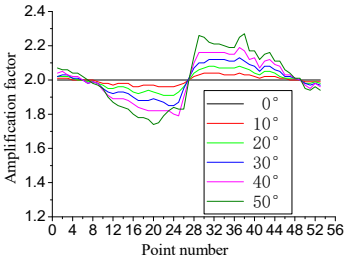

(c) Ninghe wave

Fig. 5 Amplification factors for X component peak of surface points for scarps with different slope angles (Slope width L=60m)

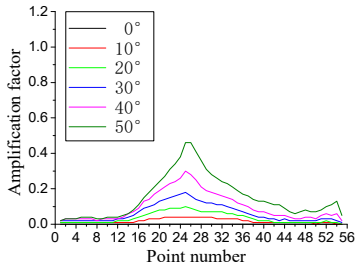

(a) Pulse wave

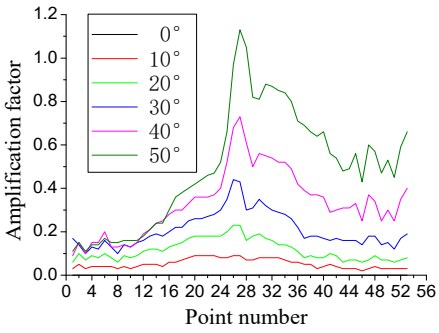

(b) El-Centro wave

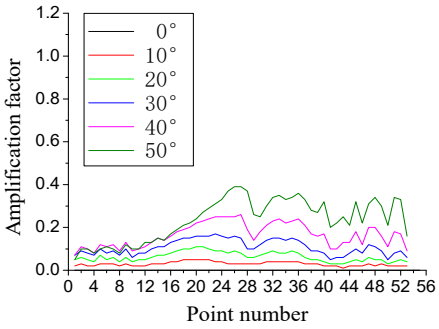

(c) Ninghe wave

Fig. 6 Amplification factors for Z component peak of surface points for scarps with different slope angles (Slope width L=60m)

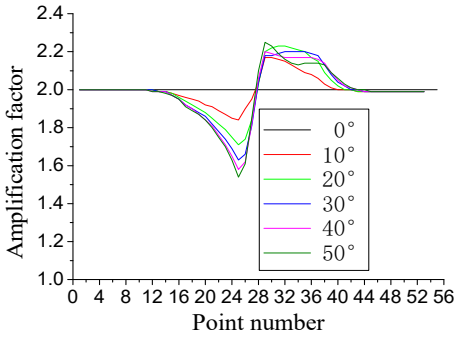

(a) Pulse wave

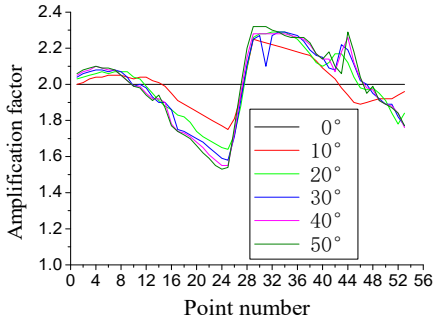

(b) El-Centro wave

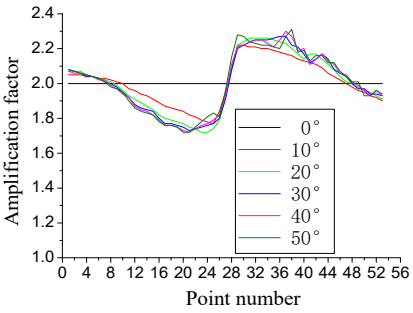

(c) Ninghe wave

Fig. 7 Amplification factors for X component peak of surface points for scarps with different slope angles (Slope height H=80m)

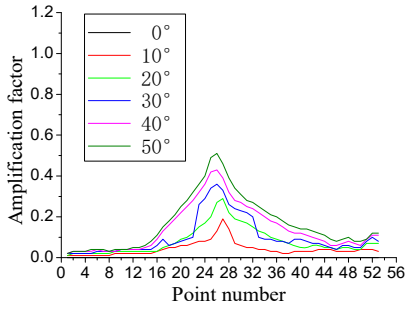

(a) Pulse wave

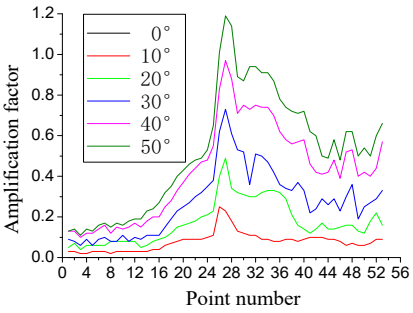

(b) El-Centro wave

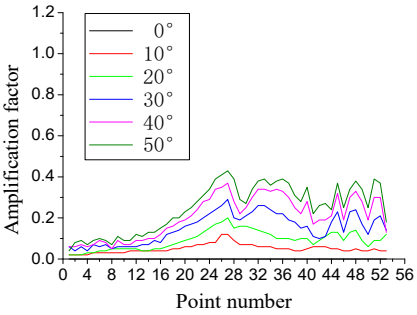

(c) Ninghe wave

Fig. 8 Amplification factors for Z component peak of surface points for scarps with different slope angles (Slope height H=80m)

1) Assumes a slope width L=60 m. Figs. 5 and 6 show the amplification factor of x and z component for the free surface stations of the scarp model for different slope

angles.

2) Assumes a slope height H=80 m. Figs. 7 and 8 show the amplification factor of x and z component for the free surface stations of the scarp model for different slope angles.
3) The influence degree of the scarp topography on surface seismic motion

It can be observed from Figs. 5 and 7 that compared with the flat surface model (its amplification factor is 2 theoretically), amplification factors at the upper side are all larger than 2, but less than 2.4. The maximum β is located at the top corner (point 29), and then decreases gradually until to the amplification factor of the flat surface model of 2.0. β of the scarp downside region is between 1.5 and 2.0, with a minimal β occurs at the lower corner (point 25). From this position to the left, the value of β increases gradually, until to a theoretical amplification factor of 2.0 for the flat surface model. From the lower corner to the upper corner, the amplification factor increases from the minimal value to the maximum value rapidly. Besides, it is shown in Figs. 5 to 7 that the results of different incident waves are similar. With the increase of slope angle, the difference between the β curves become larger, which is due to the interference between the converted wave generated at the slope surface and the free surface responses.

Generally, for a flat half-space model, there is no response for the z component when SV wave is input vertically. However, it is shown in Figs. 6 and 8 that the z component seismic motion at the scarp surface is quite strong, and becomes stronger with increasing slope angle; the closer to the scarp corner, the stronger the seismic motion. In addition, it also can be observed from Figs. 5-8 that for the x component, β of the scarp upside region (point 29 - 53) increases with growing slope angle. However, β of the scarp downside region (point 1 - 25) decreases in contrast. For the z component, the amplification factor increases obviously with the growing slope angle for both the scarp downside and upside region.

4) The influence range of the scarp topography on surface seismic motion

It is shown in Fig. 5 that when the slope width equals to 60 m, the slope angle has almost no effect on the influence range at the scarp downside region, and it is about 320 m (at point 13). The most influenced position locates at the lower corner. However, the influence range of the scarp upside region becomes larger as the slope angle increases. For instance, when slope angle changes from 10° to 50°, the influence range increases from 280 m to 500 m. The most influenced position locates at the upper corner.

It is shown in Fig. 7 that when the slope height is equal to 80 m, the slope angle also has almost no effect on the influence range at the scarp downside region, and it is about 280 m (at point 11). The most influenced position is located at the lower corner. However, the influence range of the scarp upside region becomes larger as the slope angle increases. For instance, when slope angle changes from 10° to 50°, the influence range increases from 240 m to 320 m. The most influenced position locates at the scarp's upper corner.

IV. Conclusions

In this study, the influence extent and range of the scarp topography on scarp's upside and downside seismic motion are discussed for different SV waves vertically inputted from the bottom and for different slope angles. The following conclusions can be drawn:

(1) The scarp topography has significant influence on the surface wave motion, leading to a larger amplification factor at the scarp's upside region and a smaller amplification factor at the scarp's downside region compared to that of the free surface. And the largest and smallest amplification factors are located at the top and bottom edge of the slope, respectively.
(2) The slope angle shows obvious effect on the ground motion of the x component. Amplification factors of the scarp upside region increase with the growing of the slope angle, while the downside region decrease in contrast.
(3) The influenced scopes of the scarp upside and downside region demonstrate different sensitivity degree on the slope angle. With the increasing of the slope angle, the influenced range of the scarp's upside part slightly increases, while the influenced range of the downside region is almost unchanged.
(4) The scarp topography leads to an obvious ground motion in the z component when SV wave is inputted vertically. And with the growing slope angle, amplification factors of both the upside and downside regions will also increase.
(5) Amplification factor of the Z component ground motion depends on the incident waves; while it is not sensitive to the incident wave for that of the x component ground motion.

References

[1] Tian Q. W., Yuan Y. F. Engineering Seismology. Beijing: Seismological Press, 2012.
[2] Hu Y. X., Sun P. S., Zhang Z. Y., et al. "Effects of site conditions on earthquake damage and ground motion". *Earthquake Engineering and Engineering Vibration*, 1980.
[3] Sun P. S., Hu Y. X., Tian Q. W., et al. Seismic intensities distribution and site effect of the Lancang-Gengma earthquake// Proceedings of the seismic intensities of Lancang-Gengma earthquake. Beijing: Science Press, 1991.
[4] Davis L. L., West L. R. "Observed effects of topography on ground motion". *Bulletin of the Seismological Society of America*, 1973, 63(1):283-298.
[5] Clough R. W., Chopra A. K. "Earthquake stress analysis in earth dams". *Journal of the Engineering Mechanics Division*, 1966, 92(2): 197- 212.
[6] Zhou Z. H., Wang Y. S., Wang W., et al. The effect of ridge topography on strong ground motion in Wenchuan Ms 8.0 earthquake: The case of Xishan Park, Zigong// Proceedings of the symposium to mark the first anniversary of the Wenchuan earthquake. Beijing: Seismological Press, 2009: 58-64.
[7] Trifunac M. D. "Scattering of plane SH-waves by a semi-cylindrical canyon". *Earthquake Engineering and Structure Dynamics*. 1973, 1(3): 267-281.
[8] Wong H. L., Trifunac M. D. "Scattering of plane SH-waves by a semi-elliptical canyon". *Earthquake Engineering and Structure Dynamics*. 1974, 3(2): 157- 169.
[9] Trifunac M. D. "Surface motion of a semi-cylindrical alluvial valley for incident plane SH waves". *Bulletin of the Seismological Society of America*, 1971, 61(6): 1755- 1770.
[10] Wong H. L, Trifunac M. D. "Surface motion of a semi-elliptical alluvial valley for incident plane SH waves". *Bulletin of the Seismological Society of America*, 1974, 64(5): 1389-1408.

[11] Cao H., Lee V. W. "Scattering of plane SH-waves by circular cylindrical canyons with variable depth-to-width ratio". *European Earthquake Engineering*, 1989, 2: 29-37.
[12] Yuan X. M. Application research of wave function expansion method in scattering of elastic wave(D). Harbin: Institute of Engineering Mechanics, China Earthquake Administration, 1994.
[13] Todorovska M., Lee V. W. "Surface motion of shallow circular alluvial valleys for incident plane SH waves: analytical solution" *Soil Dynamics and Earthquake Engineering,* 1991, 10(4): 192- 200.
[14] Lee V. W., Sabban M. S., GHOSH T. "3-D surface motion of long semi-circular longitudinal canyons: incident plane P waves". *European Journal of Earthquake Engineering,* 1996, 9(3): 12–22.
[15] Liang J. W., Yan L. J., Qin D., et al. "Dynamic response of circular-arc sedimentary valley site under incident plane SV wave". *China Civil Engineering Journal*, 2003, 36(12): 74–82.
[16] Liang J. W., Yan L. J., Li J. W., et al. "Response of circular- arc alluvial valleys under incident P wave". *Rock and Soil Mechanics*, 2001, 22(2):138–143.
[17] Qi S. W. "Two patterns of dynamic responses of single- free-surface slopes and their threshold height". *Chinese Journal of Geophysics,* 2006, 49(2) 518- 523.
[18] Chai H. B., Cao P., Lin H. "Dynamic response laws of slope under vertical shear wave". *Journal of Central South University* (Science and Technology), 2011, 42(4):1079- 1084.
[19] Che W., Luo Q. F. "Seismic wave propagation in complex topography". *Chinese Journal of Geotechnical Engineering*, 2008, 30(9) : 1333-1337.
[20] Ashford S. A, Sitar N. "Analysis of topographic amplification of inclined shear waves in a steep coastal bluff". *Bulletin of the Seismological Society of America,* 1997, 87(3): 692–700.
[21] Ashford S. A, Sitar N., Lysmer J., et al. "Topographic effects on the seismic response of steep slopes". *Bulletin of the Seismological Society of America*, 1997, 87(3): 701–709.